Journal of the Korean Magnetic Resonance Society **2014**, *18*, 52-57
DOI 10.6564/JKMRS.2014.18.2.052

Temperature dependent hydrogen exchange study of DNA duplexes containing binding sites for Arabidopsis TCP transcription factors

Hee-Eun Kim, Yong-Geun Choi, Ae-Ree Lee, Yeo-Jin Seo, Mun-Young Kwon, and Joon-Hwa Lee*

Department of Chemistry and Research Institute of Natural Sciences, Gyeongsang National University, Jinju, Gyeongnam 660-701, Korea

Received Sep 4, 2014; Revised Sep 22, 2014; Accepted Sep 26, 2014

Abstract The TCP domain is a DNA-binding domain present in plant transcription factors and plays important roles in various biological functions. The hydrogen exchange rate constants of the imino protons were determined for the three DNA duplexes containing the DNA-binding sites for the TCP11, TCP15, and TCP20 transcription factors using NMR spectroscopy. The M11 duplex displays unique hydrogen exchange property of the five base pairs in the first binding site (5'-GTGGG-3'). However, the M15 and M20 duplexes lead to clear changes in thermal stabilities of these five base pairs. The unique dynamic features of the five base pairs in the first binding site might play crucial roles in the sequence-specific DNA binding of the class I TCP transcription factors.

Keywords NMR, DNA binding, Hydrogen exchange, TCP transcription factor, base pair stability

Introduction

The TCP domain is a DNA-binding domain that is present in a family of plant transcription factors and consists of three characterized members of the family: TB1 (teosinte branched 1) from maize, CYC (cycloidea) from Antirrhinum and PCF from rice.1,2 On the basis of sequence homology, TCP transcription factors are able to be divided into two classes, named I and II.2 Thirteen out of 24 TCP family members from Arabidopsis belong to the class I TCP family.2 Class I TCP proteins are involved in pollen development (TCP16),3 regulating embryonic growth potential (TCP14),4 plant development (TCP20),5 and the circadian clock (TCP21).6 Recently, in vitro selection experiments revealed that Arabidopsis class I TCP proteins interact with a dyad-symmetric sequence composed of two 5'-GTGGG-3' half-sites.7 Among class I TCP proteins, TCP15 and TCP20 are able to bind to non-palindromic binding sites with preferences for 5'-GTGGGNCCNN-3', where N is any base.7 However, TCP11 showed a different DNA-binding specificity, with a preference for 5'-GTGGGCCNNN-3'.7 To understand the DNA binding mechanism of class I TCP transcription factors, the imino proton exchange rates were measured for the DNA duplexes containing the palindromic two 5'-GTGGG-3' half-sites (referred to as M11, in Fig. 1). To further understand the correlation between the base pair stabilities/dynamics and DNA binding affinities of the class I TCP transcription factors, these data were compared with

* Address correspondence to: Joon-Hwa Lee, Department of Chemistry and Research Institute of Natural Sciences, Gyeongsang National University, Jinju, Gyeongnam 660-701, Korea, Tel: 82-55-772-1490; Fax: 82-55-772-1489; E-mail: joonhwa@gnu.ac.kr

those of the DNA duplexes containing the consensus DNA-binding sites for the TCP15 and TCP20 proteins (referred to as M15 and M20, respectively, in Fig. 1), which display different binding affinities for TCP11.

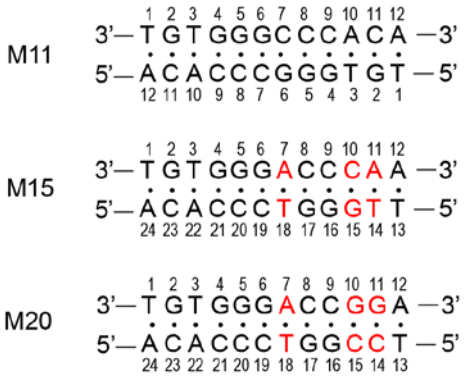

Figure 1. DNA sequence contexts of the M11, M15, and M20 DNA dodecamer duplexes.

Experimental Methods

All DNA oligonucleotides were purchased from M-biotech Co. (Seoul, Korea). The oligonucleotides were purified by reverse-phase HPLC and desalted by Sephadex G-25 column. DNA duplexes were prepared by dissolving two strands at a 1:1 stoichiometric ratio in a 90% H_2O/10% D_2O NMR buffer containing 10mM sodium phosphate (pH 8.0) and 100mM NaCl. NMR experiments were carried out on a Agilent DD2 700 MHz spectrophotometer (GNU, Jinju) equipped with *x*,*y*,*z*-axis pulsed-field gradient cold probe. One-dimensional (1D) NMR data were processed and analyzed with the program FELIX2004 (FELIX NMR, CA) or VNMRJ (Agilent, CA) and 2D data were processed with the program NMRPIPE[8] and analyzed with the program Sparky.[9] The exchange rates of the imino protons were determined as previously described.[10] The hydrogen exchange rates of the imino protons were measured by water magnetization transfer experiments.[10] The imino hydrogen exchange rate constants (k_{ex}) were determined by fitting the data to Eq. (1):[10]

$$\frac{I(t)}{I_0} = 1 - 2\frac{k_{ex}}{(R_{1w} - R_{1a})}(e^{-R_{1a}t} - e^{-R_{1w}t}) \quad (1)$$

where R_{1a} and R_{1w} were the independently measured and are the apparent longitudinal relaxation rates of the imino proton and water, respectively, and I_0 and $I(t)$ are the peak intensities of the imino proton in the water magnetization transfer experiments at times zero and t, respectively.[10]

Results and Discussion

The resonance assignment of the imino proton spectra of the M11 duplex was previously reported.[11] 2D NOESY spectra at 5 °C were used to assign the imino proton resonances of the M15 and M20 duplexes. Fig. 2 shows temperature-dependent imino proton spectra of the M11, M15, and M20 DNA duplexes. In all three duplexes, all imino proton resonances except terminal imino proton resonances could be observed at 5 °C. Most G imino proton resonances were observed up to 55 °C, indicating that these DNA duplexes are relatively stable at ≤ 55 °C. The T3 imino proton resonances were broadened at 45 °C and then disappeared as temperature was increased up to 55°C, indicating instability of the T3·A22 base pairs.

The chemical shift is sensitive to the chemical environment of the observing nuclei and to temperature-associated structural or dynamic changes. As the temperature was increased, significant crosspeak movements were observed in the imino proton spectra of the M11, M15, and M20 duplexes (*see* Fig. 2). Fig. 3 shows the temperature gradients of imino proton chemical shifts ($\Delta\delta/\Delta T$) as a function of base-pair position. In all three DNA duplexes, the A·T base pairs have significantly more negative $\Delta\delta/\Delta T$ values compared to the G·C base pairs. This indicates that the A·T base pairs are less stable and their imino protons are more rapidly exchanged with solvent water than those of the G·C base pairs. In contrast to the M11 duplex, the G6·C19 base pairs in M15 and M20 have significantly less negative $\Delta\delta/\Delta T$

values (Fig. 3), even though the G6·C19 base pair in the M15 and M20 duplexes has the neighboring

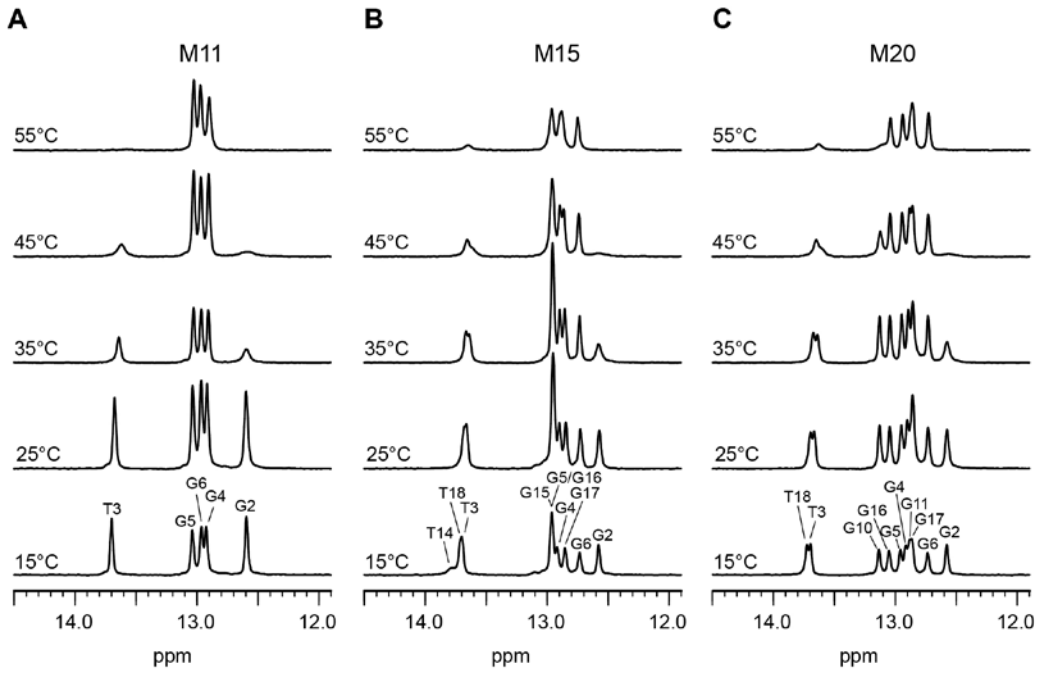

Figure 2. Temperature dependence of the imino proton resonances of the ^{1}H-NMR spectra for the (A) M11, (B) M15, and (C) M20 DNA duplexes. The experimental temperatures are shown on the left of each spectrum.

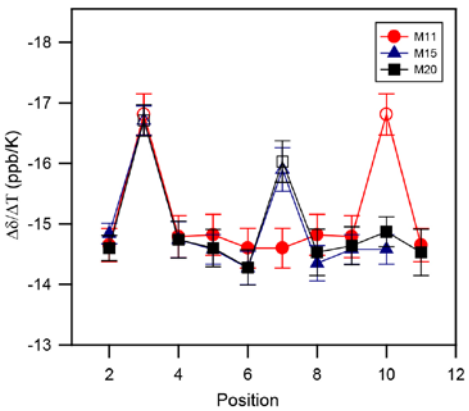

Figure 3. The $\Delta\delta/\Delta T$ values of imino proton resonances of the M11 (circle), M15 (triangle), and M20 (square) duplexes as a function of base-pair position. The closed and open symbols indicate the G·C and A·T base pairs, respectively.

A7·T18 base pair instead of the C·G base pair. These results demonstrated that the A·T base pair at position 7 more stabilizes the neighboring G6·C19 base pair than the corresponding G·C base pair. This effect propagated to the G5·C20 base pair but had little or no effect on the G4·C21 and T3·A22 base pairs (Fig. 3).

The exchange rate constants of the imino protons for the M11, M15, and M20 duplexes were determined by water magnetization transfer method at 35 ^{o}C. In the M11 duplex, the k_{ex} values of the G4 and G5 imino protons are slightly smaller than that of the G6 imino proton (Table 1), indicating that the G4·C9 and G5·C8 base pairs are relatively more stable than the G6·C7 base pair. The G2 and T3 imino protons next to the terminal base pairs show severely line-broadening and have k_{ex} of 119 ± 5 s^{-1}

and 46.8± 0.7 s^{-1}, respectively.

smaller k_{ex} value for the G6 imino proton than that of

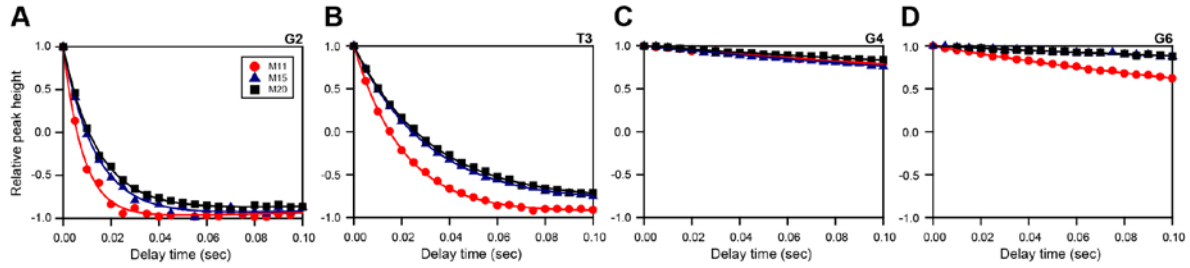

Figure 4. Relative peak height [$I(t)/I_0$] in the water magnetization transfer spectra for the (A) G2, (B) T3, (C) G4, and (D) G6 imino protons of the M11 (circle), M15 (triangle), and M20 (square) duplexes as a function of delay time. Solid lines indicate the best fitting of these data using Eq. (1).

Table 1. Hydrogen exchange rate constants (s^{-1}) of the imino protons for the M11, M15, and M20 DNA duplexes at 35°C.

Imino	M11	M15	M20
G2	109±1	72.2±2.5	65.5±1.3
T3	46.5±0.2	29.7±0.3	28.1±0.5
G4	1.1±0.1	1.4±0.2	1.1±0.2
G5	1.0±0.1	4.0±0.9[a]	0.8±0.2
G6	2.4±0.1	0.7±0.2	0.7±0.4
T18		21.5±0.4	22.0±0.3
G17		2.2±0.2	2.2±0.5
G16		4.0±0.9[a]	0.9±0.4
G10/G15		4.0±0.9[a]	6.4±0.3
G11/T14		n.a.[b]	n.d.[c]

[a]The G5, G16, and G17 resonances in the M15 duplex overlap.

[b]The T14 resonance was disappeared at 35 °C.

[c]Not determined.

In the M15 duplex, where the C·G base pair at position 7 and the AC/GT step at position 10/11 is changed to A7·T18 base pair and CA/TG step, respectively (*see* Fig. 1), the peak intensity of the G6 imino proton shows much smaller dependence on the delay time after selective water inversion compared to the M11 duplex (Fig. 4D). This leads to a 3-fold the M11 duplex (Table 1).

This demonstrates that the A7·T18 base pair more stabilizes the neighboring the G6·C19 base pair than the corresponding G·C base pair. Interestingly, the relative stability of the G6·C19 base pair induces the thermal stability of the T3·A22 and G2·C23 base pairs and the k_{ex} for T3 and G2 are 2-fold smaller than those of the M11 duplex (Fig. 4 and Table 1). However, there is no significant difference on the k_{ex} value of G4 imino proton between two duplexes (Fig. 4C and Table 1). In addition, the k_{ex} values of G5 imino proton could not be determined exactly because its resonance overlapped with G15 and G16 imino resonances (Fig. 2B).

Hydrogen exchange experiments were also performed at 35 °C for the M20 duplex, where the C·G base pair at position 7 and the AC/GT step at position 10/11 is changed to A7·T18 base pair and GG/CC step, respectively (*see* Fig. 1). Like M15, the G6 imino proton has 3-fold smaller k_{ex} value than that of the M11 duplex (Fig. 4D and Table 1). The similar result was also observed on the k_{ex} value for the G5 imino proton (Table 1). These results demonstrate that the change from G·C to A·T base pair at position 7 leads to stabilization of two neighboring G·C base pairs, although the A7·T18 base pair is more unstable than the corresponding C·G base pair in the M11 duplex. Similar to M15, the k_{ex} values for T3 and G2 are 2-fold smaller than those of the M11 (Fig. 4 and Table 1).

The linear correlation between ln(k_{ex}) and 1/T indicates the Arrhenius equation, and the slopes and y-intercepts of these lines yield the activation energies ($\Delta G_0^{\ddagger}$) and Arrhenius constants (A) of the hydrogen exchange process. The $\Delta G_0^{\ddagger}$ values for hydrogen exchange of the G2 and T3 imino protons in M11 are 25.6 and 26.8 kcal·mol^{-1}, respectively (Table 2). The G2 imino protons in M15 and M20 have significantly smaller $\Delta G_0^{\ddagger}$ compared to the M11 duplex (Table 2). The similar result was also observed on the $\Delta G_0^{\ddagger}$ values for the T3 imino proton (Table 2). These data indicate that the subtle changes at the second binding sites (5'-CCCAC-3') decrease the activation energies ($\Delta G_0^{\ddagger}$) for hydrogen exchange of the first binding site (5'-GTGGG-3'). Interestingly, the Arrhenius constants of the G2 imino protons in the M15 and M20 duplexes are 30- and 300-fold smaller than that of the M11 duplex (Table 2). The M15 and M20 duplexes also have significantly smaller A values for T3 imino than the M11 duplex (Table 2). These Arrhenius constants indicate that these imino protons in M15 and M20 are well protected from collision with solvent water molecules compared to the M11 duplex.

Table 2. The activation energies ($\Delta G_0^{\ddagger}$, kcal·mol^{-1}) and Arrhenius constants (A, s^{-1}) for hydrogen exchange of the imino protons in the M11, M15, and M20 DNA duplexes at 35°C.

		M11	M15	M20
$\Delta G_0^{\ddagger}$	G2	25.6±0.5	23.6±0.6	22.5±0.5
	T3	26.8±0.3	20.4±0.4	19.2±0.5
A ($\times 10^{18}$)	G2	146±3	4.4±0.1	0.5±0.1
	T3	443±5	0.0095±0.0002	0.0011±0.0001

The SELEX study revealed that class I transcription factors (TCP11, TCP15, and TCP20) efficiently recognized the palindromic consensus binding site, 5'-GTGGGCCCAC-3' (M11 sequence).[7] EMSA competition assay study found that the subtle changes of the second binding site, 5'-CCCAC-3', did not affect the DNA binding affinity of TCP15 and TCP20.[7] Interestingly, TCP15 and TCP20 is able to bind efficiently both the M15 and M20 sequences, even though these two duplexes contain different sequences at the second binding site (M15: 5'-ACCCA-3' and M20: 5'-ACCGG-3').[7] This can be explained by our observation that the M15 and M20 duplexes have the same hydrogen exchange properties of the five base pairs in the first consensus binding site (5'-G2T3G4G5G6-3'). However, the TCP11 protein shows significantly lower binding affinities for M15 and M20 compared to the consensus M11 duplex.[7] Our hydrogen study found that, unlike M15 and M20, the M11 duplex showed the clear differences in the hydrogen exchange process of the first consensus binding site. Thus, we can conclude that the unique dynamic features of the five base pairs in the first consensus binding sequence might play crucial roles in the DNA binding as well as sequence specificity of various class I TCP proteins.

In summary, we determined the k_{ex} values of the imino protons in the three DNA duplexes containing the DNA-binding sites for the TCP11, TCP15, and TCP20 transcription factors using NMR spectroscopy. The M11 duplex displays unique hydrogen exchange property of the five base pairs in the first binding site (5'-GTGGG-3'). However, the M15 and M20 duplexes lead to clear changes in thermal stabilities of these five base pairs. These unique dynamic features of the five base pairs in the first binding site might play crucial roles in the sequence-specific DNA binding of the class I TCP transcription factors.

Acknowledgements

This work was supported by the National Research Foundation of Korea Grants [2010-0020480 and 2013-R1A2A2A05003837] funded by the Korean Government (MEST). This work was also supported by a grant from Next-Generation BioGreen 21 Program (SSAC, no. PJ009041), Rural Development Administration, Korea. We thank the GNU Central Instrument Facility for performing the NMR experiments.

References

1. P. Cubas, N. Lauter, J. Doebley, and E. Coen, *Plant J.* **18**, 215. (1999).
2. M. Martin-Trillo and P. Cubas, *Trends Plant Sci.* **15**, 31. (2010)
3. T. Taketa, K. Amano, M. Ohto, K. Nakamura, S. Sato, T. Kato, S. Tabata, and C. Ueguchi, *Plant Mol. Biol.* **61**, 165. (2006).
4. K. Tatematsu, K. Nakabayashi, Y. Kamiya, and E. Nambara, *Plant J.* **53**, 42. (2008).
5. C. Herve, P. Dabos, C. Bardet, A. Jauneau, M. C. Auriac, A. Ramboer, F. Lacout, and D. Tremousaygue, *Plant Physiol.* **149**, 1462. (2009).
6. J. L. Pruneda-Paz, G. Breton, A. Para, and S. A. Kay, *Science* **323**, 1481. (2009).
7. I. L. Viola, N. G. Uberti Manassero, R. Ripoll, and D. H. Gonzalez, *Biochem. J.* **435**, 143. (2011).
8. F. Delaglio, S. Grzesiek, G. W. Vuister, G. Zhu, J. Pfeifer, and A. Bax, *J. Biomol. NMR* **6**, 277. (1995).
9. T. D. Goddard and D. G. Kneller, SPARKY 3. University of California, San Francisco, CA. (2003).
10. J.-H. Lee and A. Pardi, *Nucleic Acids Res.* **35**, 2965. (2007).
11. Y.-G. Choi, H.-E. Kim, J.-H. Lee, *J. Korean Magn. Reson. Soc.* **17**, 76. (2013).